

Automatic Skin Lesion Segmentation based on Saliency and Color

Giuliana Ramella ^a

Institute for the Applications of Calculus "M. Picone", CNR, Via P. Castellino 111, 80131 Naples, Italy

Keywords: Dermoscopic Images, Color Image Processing, Saliency Map, Skin Lesion Segmentation.

Abstract: Segmenting skin lesions in dermoscopic images is a key step for the automatic diagnosis of melanoma. In this framework, this paper presents a new algorithm that after a pre-processing phase aimed at reducing the computation burden, removing artifacts and improving contrast, selects the skin lesion pixels in terms of their saliency and color. The method is tested on a publicly available dataset and is evaluated both qualitatively and quantitatively.

1 INTRODUCTION

Melanoma is an aggressive skin cancer, which is caused by an uncontrolled growth of abnormal cells (melanocytes cells). It is likely to be lethal. However, if detected at the initial stage, melanoma can be treated by means of surgical eradication of the cancerous cells with high cure rate. Thus, early diagnosis is the best way to reduce the number of deaths caused by melanoma.

Visual examination of the skin surface is a simple way for melanoma detection that, however, has a limited accuracy especially at earlier stages of the illness. Thus, dermatologists resort to the use of an imaging technique (called dermoscopy or epiluminescence microscopy) that by eliminating surface reflection allows to visually enhance deeper skin layers. To this purpose, a tool called dermatoscope is employed, which consists of a magnifying glass, a (polarized or non-polarized) light source, and a transparent plate. The dermatoscope can be contact or non-contact and in the first case some dermoscopic oil or gel is applied on the skin before using the instrument.

By analyzing the dermoscopic images, expert dermatologists are able to distinguish malignant and benign lesions by assigning to each lesion a score in terms of four principal features (the ABCD rule): asymmetry, border, color and differential structures. However, the diagnosis is likely to be biased by the subjective judgment of the doctor, who may not have

enough experience, and is limitedly reproducible. Thus, to reduce the number of deaths from melanoma, the development of innovative fully automatic techniques for segmentation, feature extraction and classification of dermoscopic images is highly desirable. Recent surveys can be found in (Premaladha et al., 2015), (Mishra et al., 2016), (Oliveira et al., 2018), (Okur et al., 2018).

Due to the effect it has on feature extraction and classification, the segmentation phase is particularly relevant. Color image segmentation is a complex task (Celebi et al. 2013, Ramella et al. 2013) due to a number of problems such as the existence of different colors within the lesion, the presence of artifacts, or the low contrast at the border separating the lesion from the surrounding healthy skin. Some artifacts, e.g., dark corners, ink markers, rulers and bubbles, are caused directly by the imaging technique, while other artifacts are due to different conditions of illumination, contrast and noise. A major problem severely affecting the correct detection of the border of the lesion is the presence of hair on the skin.

All artifacts should be removed before applying the segmentation algorithm. Thus, almost all dermoscopic image analysis methods include a pre-processing step aimed at removing the artifacts. Median filtering, e.g. (Mendonca et al., 2015), color correction, e.g. (Quintana et al., 2011), illumination correction, e.g. (Glaister et al., 2013), contrast enhancement, e.g. (Abbas et al., 2013), (Barata et al., 2015), and hair removal, e.g. (Lee et al., 1994), are

^a <http://orcid.org/0000-0001-6044-5237>

often employed. Unfortunately, the best that pre-processing can do is to reduce the effect of the artifacts, which only seldom are completely removed. Thus, a post-processing step is also generally taken into account, e.g., based on region merging or morphological operations.

Automated skin lesion segmentation has received a lot of attention in the recent literature, where a number of segmentation methods based on different approaches can be found. The most common and simple automatic segmentation methods are based on thresholding the histogram based on RGB channels, luminance, or principal component analysis (Garnavi et al., 2011), (Celebi et al., 2013), (Zortea et al., 2017). Unfortunately, thresholding methods are limited by the distribution of the luminance and may fail in the presence of multiple peaks in the luminance histogram. Other methods involve deformable models, such as active contours, (Ma et al., 2016), (Celebi et al., 2017). Generally speaking, the strategy consists in the identification of an optimum boundary of the skin lesion by minimizing the internal forces defined within the curve and the external energies. The main problems with deformable models concern the selection of the segmentation parameters and the unnecessary computations caused by the presence of a non adequate stopping criterion. Region based segmentation has also been used for dermoscopic images (Celebi et al., 2007), (Celebi et al., 2008), (Celebi et al., 2009), where predefined features such as color, intensity, wavelets are employed to divide the image at hand into distinct regions. Good results have been obtained by using supervised learning approaches such as convolutional neural networks (CNNs) that, however, require extensive learning based on a very large number of parameters and of labeled training images (Kawaraha et al., 2016), (Codella et al., 2015), (Yu et al. 2017). Other recent methods such as (Ahn et al., 2015), (Ahn et al. 2017), (Fan et al., 2017), (Hu et al., 2019), are based on saliency detection to identify visually salient regions as those that are visually more distinctive due to their contrast.

In this paper we introduce a new dermoscopic image segmentation method that consist of a pre-processing step aiming at preparing the image and a successive process to identify the skin lesion in terms of visual appearance and color.

To evaluate the performance of the method we have applied it to dermoscopic images in the publicly available dataset (ISIC, 2016), as done by many researchers active in dermoscopic image analysis.

2 THE METHOD

To describe the main steps of the suggested method we consider as running example one of the images in the ISIC database (ISIC, 2016), namely image ISIC_0000003 shown in Figure 1 left. The ground truth provided in the database is shown in Figure 1 middle.



Figure 1: Image ISIC_0000003 used as running example, left, the corresponding ground truth, middle, and the quantized image, right.

2.1 Image Preparation

The first step is Image Preparation. To limit the computation burden of the segmentation process, we reduce the size of the images as well as the number of colors. To reduce the size of the image in such a way that the maximum between the number of rows and the number of columns is 500. See the result for the running example in Figure 1 right. The same size reduction is also done for the ground truth. To reduce the number of colors, we perform image quantization. Different color quantization methods can be used to this purpose (e. g. Dekker, 1994, Bruni et al., 2015, Ramella et al., 2016). In this paper we use the algorithm in (Dekker, 1994) and set to 64 the maximum number of colors.

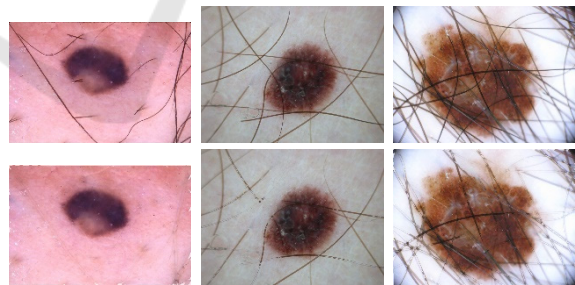


Figure 2: Images ISIC_0000177, ISIC_0000138 and ISIC_0000043 characterized by the presence of hair, top, and the resulting images after hair removal by the algorithm in (Lee et al, 1997), bottom.

Finally, we apply the hair removal process by the algorithm in (Lee et al, 1997) in order lesion images can be more effectively segmented after the hair present in the lesion image is removed and the portion of the image in correspondence with the removed hair is restored. Unfortunately, hair removal is not always completely successful. See Figure 2, showing one

example where hair removal has been completely successful and other two examples where it has not.

2.2 Saliency Map Construction and Preliminary Segmentation

The successive step of the process is Saliency Map Construction and Processing. We resort to the algorithm suggested in (Achanta et al., 2009) that computes full resolution saliency maps with well-defined boundaries of salient objects. To enhance the obtained saliency map, we increase the contrast by mapping the values of the input intensity image to new values obtained by saturating the bottom 1% and the top 1% of all pixel values. Figure 3 shows the saliency map computed for the running example and the resulting image after contrast enhancement.

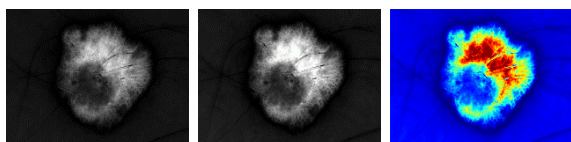


Figure 3: Saliency map before, left, and after contrast enhancement, middle. The latter image is also shown in false colors for better visualization, right.

The saliency map undergoes binarization to extract the more salient regions: all pixels with saliency value smaller than the average saliency value are tentatively assigned to the background, while all other pixels are tentatively assigned to the foreground. We observe that for a number of images the average saliency value is strongly conditioned by artifacts caused directly by the adopted imaging technique. This the case, for example, in the presence of dark corners (see Figure 4 left) or, even worse, when the region of interest for saliency map thresholding constitutes a circular portion of an otherwise completely dark image. In the presence of these dark artifacts, which are characterized by rather high saliency value (see Figure 4 right), the average saliency value would be higher than the average saliency value actually characterizing the pixels in the skin lesion. As a consequence, the number of pixels that would be assigned to the foreground is remarkably smaller than expected. For this reason, saliency map thresholding involves a process aimed at identifying a Binary Mask including all pixels whose saliency value should not be taken into account for average saliency value computation. Moreover, an iterated process is actually performed to identify the Binary Mask since not all pixels of the artifacts are characterized by the same (high) saliency value.

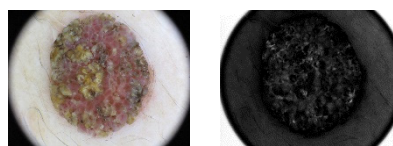


Figure 4: Image ISIC_0000101 characterized by dark artifacts due to the imaging technique, left, and its corresponding saliency map, where the average saliency value is strongly conditioned by the high values (shown in white) associated with the dark artifacts, right.

At each iteration, the saliency map is binarized with the current threshold value. Then, connected components including pixels on the image frame are removed from the saliency map, i.e., their pixels are set to zero, and are recorded in a Binary Mask image. The average saliency value is newly computed by ignoring the pixels whose saliency has been set equal to zero. Generally, a smaller average saliency value is obtained so that, when the saliency map is thresholded again, a larger number of pixels overcome the new threshold, which are selected as potentially belonging to the foreground. The process for saliency map binarization and Binary Mask construction is iterated as far as connected components including pixels of the frame are detected. As an example, refer to Figure 5.

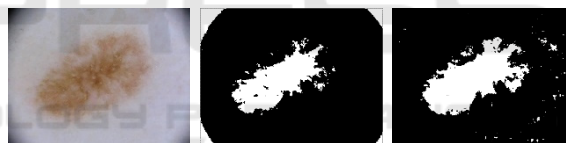


Figure 5: Image ISIC_000014, left, the binarized saliency map with components including pixels of the frame, middle, and the result at the successive iteration, where a larger number of pixels overcome the new, lower, threshold, right.

Another relevant process of the saliency map is likely to be necessary for images where the background, normally lighter than the foreground, includes some regions that are lighter than the remaining background regions. Since salient regions are regions visually more evident than the surrounding areas, it may happen that both pixels inside the lesion, hence characterized by darker colors, and pixels in the lightest portions of the background have saliency values high enough to be potentially assigned to the foreground during binarization. See Figure 6.

To solve the above problem, we consider the colors of the pixels corresponding to foreground pixels in the binarized saliency map and compute the average color associated to each connected component of the binarized saliency map. Then, we

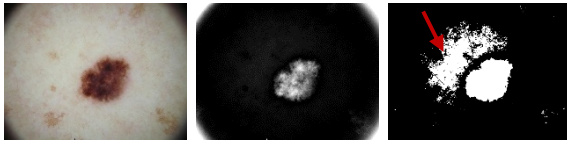


Figure 6: Image ISIC_0011298, left, the initial saliency map, middle, and the binarized saliency map where the component pointed by the arrow should not be assigned to the foreground.

identify among the computed average colors, the color having the minimal (maximal) distance d_{min} (d_{max}) from the darkest detected color and compute the difference $d_{max}-d_{min}$. We observe that when the components in the saliency map are characterized by rather different average colors, the difference $d_{max}-d_{min}$ is large. If this is the case, we remove from the foreground the too light components, i.e., the components characterized by an average color larger than the mean value between d_{min} and d_{max} .

For the running example, the saliency map obtained at the end of the iterated binarization is shown in Figure 7 left.



Figure 7: Saliency map at the end of the iterated binarization, left, and after pixels with lower saliency but adequate color have been assigned to the foreground, right.

We remark that skin lesions may include pixels with different colors, but in any case the difference in color between foreground and background is still noticeable. Thus, we accept as belonging to the foreground also some pixels characterized by low saliency values that prevented their extraction during thresholding, provided that their colors are closer to the average color of the foreground than to the average color of the background. For the running example the resulting image is shown in Figure 7 right.

The binarized saliency map is likely to consist of a number of components, all characterized by saliency or color compatible with those expected for the skin lesion to be segmented. However, not all these components do belong to the skin lesion. Some peripheral parts can be just noisy regions characterized by saliency or color very similar to those in the skin lesion. To keep only the relevant components, we distinguish all components in kernel and non-kernel components. Kernel components are those including pixels with the highest saliency

values. Non-kernel components include pixels with saliency lower than the binarization threshold, or pixels with saliency sufficiently high to guarantee their detection during binarization, but barely overcoming the threshold value. Non-kernel components with very small area or with area larger than the total area of the kernel components are assigned to the background. For each other non-kernel component, its proximity to the kernel is evaluated as the difference in area between the convex hull of the set consisting of the kernel components plus the non-kernel component at hand, and the convex hull of the kernel components. A small difference indicates that the non-kernel component is sufficiently close to the kernel to be accepted in the foreground. An example is shown in Figure 8.

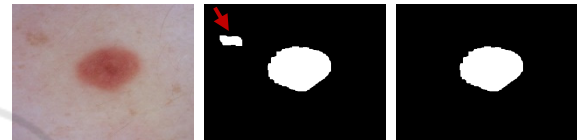


Figure 8: Image ISIC_0000092, left, the binarized saliency map where the only non-kernel component is pointed by the arrow, middle, and the result after the assignment of the non-kernel component to the background, right.

2.3 Final Segmentation

In many cases, the segmented foreground obtained at the end of the previous step is already close enough to the desired result. However, there are skin lesions for which the transition in color from foreground to background is not sharp. In these cases, a sort of band surrounding the detected foreground can be noted in the saliency map. The band includes pixels that have low saliency values, say smaller than 10, but have rather different colors. These colors are light for pixels really belonging to the background, while are a bit darker for pixels belonging to the skin lesion in the color transition area. Thus, an expansion of the foreground is necessary to include some pixels selected out of those placed in the band surrounding the current foreground. To this aim, we perform the following process. We select from the original saliency map the band, consisting of the pixels with saliency smaller than 10 (see Figure 9 left). Then, we compute the average color c_F of the current foreground, the average color c_B of the band and the distance d between c_F and c_B . We use d to filter out from the band the pixels that cannot absolutely be assigned to the foreground. Our choice is to filter out band pixels whose colors have distance from c_F larger than the 80% of d (see Figure 9 middle). Then, out of

the remaining pixels, only those connected to the already detected foreground are assigned to the foreground (see Figure 9 right).

For the running example (Figure 9 top), the set of band pixels assigned to the foreground coincides with the set of filtered pixels. In Figure 9 bottom, we provide a second example, where the selected pixels are a subset of the filtered band pixels.

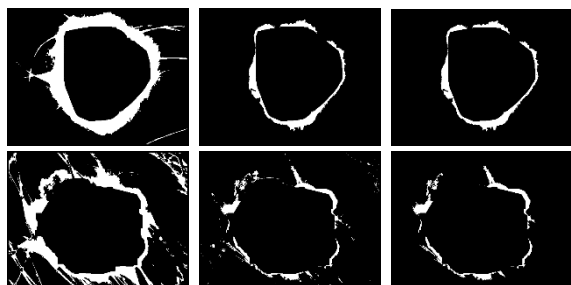


Figure 9: Expansion of the foreground for the running example, top, and for image ISIC_000043, bottom. Band pixels, left, pixels remaining after filtering, middle, and pixels assigned to the foreground, right.

Morphological operations are applied to smooth the contour of the segmented skin lesion and fill possibly existing small holes. If more than one component is obtained, the one with the largest area is selected. The convex hull of such a component is finally computed and constitutes the result of segmentation.

In Figure 10, the result of segmentation for the running example is shown.



Figure 10: Detected boundary of the segmented skin lesion superimposed onto the input, left, and comparison of the segmentation result with the ground truth, right, where white is used for True Positive pixels, red for False Positive pixels and green for False Negative pixels.

3 EXPERIMENTAL RESULTS

We have tested our method on the publicly available dataset of dermoscopic images ISIC (ISIC, 2016). ISIC is one of the largest archive of quality controlled dermoscopic images of skin lesions and is kept by the International Skin Imaging Collaboration (ISIC) with the aim of improving melanoma diagnosis. Every year the archive is updated by adding the ground truth images for the test images of the previous year

challenge as well as a new set of images. The ISIC 2016 database we have used for the experimental work of this paper includes images representative of both malignant and benign skin lesions. For each of these images, the ground truth is also available.

3.1 Qualitative Evaluation

The results of the proposed segmentation method can be seen in Figure 11, where some examples are shown.

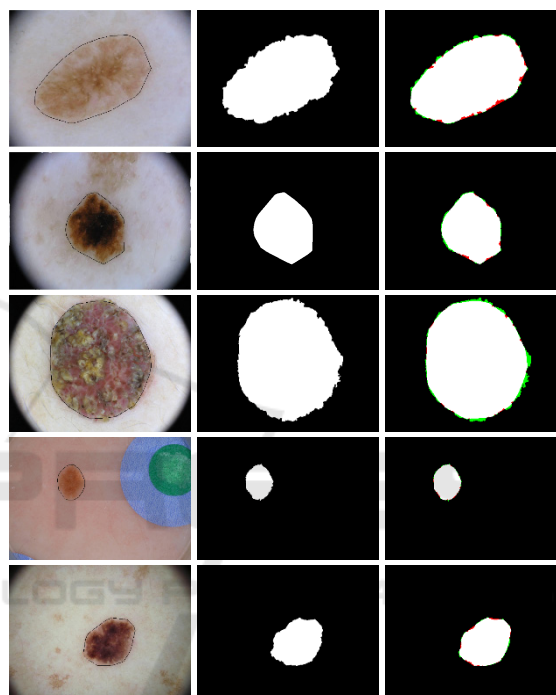


Figure 11: From top row to bottom row, results for images ISIC_0000014, ISIC_0000072, ISIC_0000101, ISIC_0005000, ISIC_0011298. Detected boundary of the segmented skin lesions superimposed on the input, left column, ground truth segmentation masks, middle column, detected skin lesions with False Positive pixels (red) and False Negative pixels (green), right column.

The segmentation method may fail to identify accurately the skin lesion when the pre-processing phase has not been sufficient to clean properly the image. This is particularly the case as regards hair removal (see Figure 2). Moreover, for a limited number of cases the non-correct obtained result is intrinsically due to the fact that we base segmentation on saliency and for some images saliency is not adequate to extract the desired foreground. As an example, see Figure 12, where the highest saliency values are found in the background while saliency value within the skin lesion is extremely low.

Finally, we would like to point out that not all ground truth images are characterized by the same high level of detail. In fact, in some ground truth images the lesion's boundary is delineated very accurately, which is typical of results obtained by an automatic segmentation software, while for other images the boundary is more roughly approximated, which is typical of segmentation manually achieved by the dermatologists. This justifies the fact that our results are sometime very close to the ground truth images, while sometimes differ more from those.

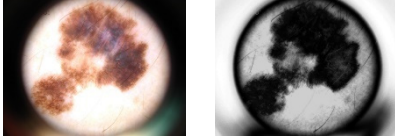


Figure 12: Image ISIC_0001131, left, and the contrast saliency map, right.

3.2 Quantitative Evaluation

To evaluate the proposed method, we have used on ISIC 2016 the following measures, as defined in (Gutman et al., 2016): pixel-level accuracy (AC), sensitivity (SE), and specificity (SP), as well as Dice coefficient (DI) and Jaccard index (JA). The average value of these measures are: AC=0.910; SE=0.832; SP=0.958; DI=0.843; JA=0.760.

Moreover, we have compared the performance of our method with that of classical saliency-based methods (Yang et al. 2013, Zhu et al. 2014, Cheng et al. 2015, Fan et al. 2017) and with that of some more recent saliency-based methods specifically applied to dermoscopic images (Ahn et al. 2015, Ahn et al. 2017, Fan et al. 2017, Hu et al. 2019) in terms of the measure used in all cited papers: the Dice coefficient (DI), defined as:

$$DI = \frac{2 * TP}{2 * TP + FN + FP}$$

where TP, FP, and FN denote True Positive, False Positive and False Negative pixels, respectively. The quantitative evaluation for the comparison with the other methods is given in Table 1, where the DI values have been taken from the cited papers or from (Ahn et al., 2017).

Table 1: Average performance results on ISIC Dataset in terms of DI.

Method	DI
Yang et al., 2013	0.807
Zhu et al., 2014	0.804
Ahn et al., 2015	0.740
Cheng et al., 2015	0.697
Ahn et al., 2017	0.834
Fan et al., 2017	0.818
Hu et al., 2019	0.824
Proposed	0.843

4 CONCLUSIONS

In this paper, we have suggested a new method based on saliency and color to segment skin lesions in dermoscopic images. The method has a first phase devoted to image preparation, during which the computation burden of the segmentation process is lowered by reducing the size of the images as well as the number of colors. Since a problem severely affecting the correct detection of the lesion is the presence of hair on the skin, the image then undergoes a hair removal process, after which the saliency map is computed. The contrast of the map is increased and, by means of an iterate process, the Binary Mask including artifacts such as dark corners is built to work only on the portion of the image including the lesion and the surrounding skin. Color information is also taken into account to ascribe to the foreground pixels that during the saliency binarization are not detected as foreground pixels due to their saliency level that is lower than the threshold. These pixels are ascribed to the foreground provided that their colors satisfy specific conditions. Then, a further process effective in all cases in which the color transition from foreground to background is not sharp is done to identify among all background pixels those that can be assigned to the foreground. Morphological operations are applied to improve the shape of the foreground. The component with maximal area is selected and its convex hull is taken as the segmentation result.

The method has been tested on a publicly available database providing satisfactory results. It has been evaluated both qualitatively, by comparing the results to the ground truth provided in the database, and quantitatively in terms of a commonly adopted measure.

In the future investigations, there is room to improve in different directions this preliminary version of the proposed method based on saliency and color. In particular, the next step will be devoted to

extensive comparative studies with the existing methods and to a generalization of the method in order to make it robust also in presence of initially not removed artifacts.

ACKNOWLEDGEMENTS

This work has been supported by the GNCS (Gruppo Nazionale di Calcolo Scientifico) of the INDAM (Istituto Nazionale di Alta Matematica).

REFERENCES

- Abbas, Q., Garcia, I.F., Celebi, M.E., Ahmad, W., Mushtaq, Q., 2013. A perceptually oriented method for contrast enhancement and segmentation of dermoscopy images, *Skin Res. Technol.* 19 (1), pp. 490–497.
- Achanta, R., Hemami, S., Estrada, F., Susstrunk, S., 2009. Frequency-tuned salient region detection. In *2009 IEEE Conference on Computer Vision and Pattern Recognition*, pp. 1507–1604.
- Ahn, E., Bi, L., Jung, Y.H., Kim, J., Li, C., Fulham, M., Feng, D.D., 2015. Automated saliency-based lesion segmentation in dermoscopic images. In *2015 37th annual international conference of the IEEE engineering in medicine and biology society (EMBC)*, pp. 3009–3012.
- Ahn, E., Kim, J., Bi, L., Kumar, A., Li, C., Fulham, M., Feng, D.D., 2017. Saliency-Based Lesion Segmentation Via Background Detection in Dermoscopic Images, *IEEE Journal of Biomedical and Health Informatics*, Vol. 21 (6), pp. 1685–1693.
- Barata C., Celebi, M.E., Marques, J.S., 2015. Improving dermoscopy image classification using color constancy, *IEEE J Biomed Health Inform* 19(3), pp. 1146–1152.
- Bruni, V., Ramella, G., Vitulano, D., 2015. Automatic Perceptual Color Quantization of Dermoscopic Images. In *VISAPP 2015*, J. Braz et al. Eds., Scitepress Science and Technology Publications, vol. 1, pp. 323–330.
- Celebi, M.E., Aslandogan, Y.A., Stoecker, W.V., Iyatomi, H., Oka, H., Chen, X., 2007. Unsupervised border detection in dermoscopy images, *Skin Res. Tech.*, vol. 13, pp. 454–462.
- Celebi, M.E., Kingravi, H.A., Iyatomi, H., Aslandogan, Y.A., Stoecker, W.V., Moss, R.H., Malters, J.M., Grichnik, J.M., Marghoob, A.A., Rabinovitz, H.S., Menzies, S.W., 2008. Border detection in dermoscopy images using statistical region merging, *Skin Res. Tech.*, vol. 14, pp. 347–353.
- Celebi, M. E. , Iyatomi, H., Schaefer, G., W.V. Stoecker, W.V., 2009. Lesion border detection in dermoscopy images, *Comput. Med. Imag. Graph.*, vol. 33, pp. 148–153.
- Celebi, M. E., Wen, Q., Hwang, S., Iyatomi, H., Schaefer, G., 2013. Lesion border detection in dermoscopy images using ensembles of thresholding methods, *Skin Res. Technol.* 19 (1), pp. 252–258.
- Celebi, M.E., Schaefer G., 2013. Color Medical Image Analysis, *Lecture Notes in Computational Vision and Biomechanics*, vol. 6.
- Cheng, M.M., Mitra N.J., Huang X., Torr P.H.S., Hu S.M., 2015. Global contrast based salient region detection. *IEEE Trans Pattern Anal Mach Intell* 37(3), pp. 569–582.
- Codella, N., Cai, J., Abedini, M., Garnavi, R., Halpern, A., Smith, J.R., 2015. Deep learning, sparse coding, and SVM for melanoma recognition in dermoscopy images, *Int. W. Mach. Learning Med. Imag.*, Vol. 9352, pp. 118–126.
- Dekker, A., 1994. Kohonen neural networks for optimal colour quantization. *Network Computation in Neural Systems*, 5(3), pp. 351–367.
- Fan, H., Xie, F., Li, Y., Jiang, Z., Liu, J., 2017. Automatic segmentation of dermoscopy images using saliency combined with Otsu threshold. *Comput Biol Med* 85:75–85
- Garnavi, R., Aldeen, M., Celebi, M. E., Bhuiyan, A., Dolianitis, C., Varigos, G., 2011. Automatic Segmentation of Dermoscopy Images Using Histogram Thresholding on Optimal Color Channels, *Int. Journal of Biomedical and Biological Engineering*, Vol. 5, No:7, pp. 275–283.
- Glaister, J., Amelard, R., Wong, A., Clausi, D., 2013. MSIM: multistage illumination modeling of dermatological photographs for illumination-corrected skin lesion analysis, *IEEE Trans Biomed Eng* 60(7), pp. 1873–1883.
- Gutman, D., Codella, N.C.F., Celebi, E., Helba, B., Marchetti, M., Mishra, N., Halpern, A., 2016. Skin lesion analysis toward melanoma detection: A challenge at the International Symposium on Biomedical Imaging (ISBI) 2016, hosted by the International Skin Imaging Collaboration (ISIC), arXiv:1605.01397 [cs.CV], 2016.
- Hu, K., Liu, S., Zhang, Y., Cao, C., Xiao, F., Huang, W., Gao, X., 2019. Automatic segmentation of dermoscopy images using saliency combined with adaptive thresholding based on wavelet transform, *Multimedia Tools and Applications*, pp. 1–18.
- ISIC, 2016. ISIC Archive : *The International Skin Imaging Collaboration: Melanoma Project*, ISIC, 5 Jan 2016. [Online]. Available: <https://isic-archive.com/#>.
- Kawaraha, J., Ben Taieb, A., Hamarneh, G., 2016. Deep features to classify skin lesions, *IEEE 13th Int. Symp. Biomed. Imag.*, pp. 1397–1400.
- Lee, T., Ng, V., Gallagher, R., Coldman, A., McLean, D., 1997. Dullrazor: A software approach to hair removal from images, *Comput. Biol. Med.* 27 (6), pp. 533–543.
- Ma, Z., Tavares, J.M.R.S., 2016. A novel approach to segment skin lesions in dermoscopic images based on a deformable model, *IEEE J. Biomed. Health Inf.*, vol. 20, no. 2, pp. 615–623.
- Mendonca, T., Ferreira, P.M., Marques, J.S., Marcal, A.R., Rozeira, J., 2015. PH2 –A public database for the analysis of dermoscopic images. In *Dermoscopy Image*

- Analysis*, Celebi, M. E., Mendonca, T., Marques, J.S., Eds., Boca Raton, CRC Press, pp. 419-439.
- Mishra, N.K., M.E. Celebi, M.E., 2016. An Overview of Melanoma Detection in Dermoscopy Images Using Image Processing and Machine Learning, arXiv:1601.07843 [cs.CV].
- Okur, E., Turkan, M., 2018. A survey on automated melanoma detection, *Eng. Applications of Artificial Intelligence*, 73, pp. 50-67.
- Oliveira, R.B., Papa, J.P., Pereira, A.S., Tavares, J.M.R.S., 2018. Computational methods for pigmented skin lesion classification in images: review and future trends, *Neural Comput. & Applic.* 29, pp. 613-636.
- Premaladha, J., Lakshmi Priya, M., Sujitha, S., K. S. Ravichandran, K. S., 2015. A Survey on Color Image Segmentation Techniques for Melanoma Diagnosis, *Indian Journal of Science and Technology*, 8(22), IPL0265.
- Quintana, J., Garcia, R., Neumann, L., 2011. A novel method for color correction in epiluminescence microscopy, *Comput. Med. Image Graph.* 35 (7), pp. 646–652
- Ramella, G., Sanniti di Baja, G., 2013. Image segmentation based on representative colors and region merging, in Pattern Recognition, Carrasco-Ochoa J. A. et al Eds., *Lecture Notes in Computer Science 7914*, Springer, pp. 175-184.
- Ramella, G., Sanniti di Baja, G., 2016. From color quantization to image segmentation. In *Proc. 12th International Conference on Signal Image Technology & Internet-Based Systems - SITIS 2016*, K. Yetongnon et al. Eds., IEEE Computer Society, pp. 798-804.
- Yang C., Zhang L., Lu H., Ruan X., Yang M.H., 2013. Saliency detection via graph-based manifold ranking. In *Proceedings of the IEEE conference on computer vision and pattern recognition*, pp. 3166–3173.
- Yu, L., Chen, H., Dou, Q., Qin, J., Heng, P. A., 2017. Automated melanoma recognition in dermoscopy images via very deep residual networks, *IEEE Trans. Med. Imaging* 36 (4), pp. 994–1004.
- Zhu W., Liang S., Wei Y., Sun J., 2014. Saliency optimization from robust background detection. In: *Proceedings of the IEEE conference on computer vision and pattern recognition*, pp 2814–2821
- Zhou, H., Li, X., Schaefer, G., Celebi, M.E., Miller, P., 2013. Mean shift based gradient vector flow for image segmentation, *Comput. Vis. Image Understanding*, vol. 117, pp. 1004–1016.
- Zortea, M., Flores, E., Scharcanski, J., 2017. A simple weighted thresholding method for the segmentation of pigmented skin lesions in macroscopic images, *Pattern Recogn.* 64, pp. 92–104.